Research Article – Vol. 02, Issue 01, No.04

Advanced in Engineering and Intelligence Systems

Journal Web Page: https://aeis.bilijipub.com

Estimation of the Compressive Strength of Self-compacting concrete (SCC) by a Machine Learning Technique coupling with Novel Optimization Algorithms

Ling Chen[1,*] , Wengang Jiang[1]

[1] *Logistics Department, Taizhou Vocational & Technical College, Taizhou, Zhejiang, 318000, China*

Highlights

- Hybrid support vector regression (SVR) models were proposed for developing prediction models to forecast the compressive strength of self-compact concrete.
- Henry's Gas Solubility Optimization (HGSO), Particle Swarm Optimization (PSO) were used.
- SVR model optimized with HGSO algorithm can be proposed as the most appropriate model.

Article Info

Received: 26 January 2023
Received in revised: 27 March 2023
Accepted: 19 March 2023
Available online: 28 March 2023

Keywords

Self-compacting concrete;
Particle Swarm Optimization;
Support vector regression;
Henry's Gas Solubility Optimization;
Compressive Strength.

Abstract

Self-compacting concrete (SCC), as a liquid aggregate, is suitable for use in reinforced constructions with no need for vibration. SCC utilization has been found in a wide range of projects. Nevertheless, those applications are often limited due to lacking the knowledge about such mixed materials, especially from experimental testing. The factor of Compressive Strength (CS), which is one of the vital mechanical variables in structure immunization, can be computed either through costly tests or predictive models. Intelligent systems can appraise CS based on ingredients' data fed to the models. This research aims to model the CS of SCC via a machine learning technique of Support Vector Regression (SVR). The Particle Swarm Optimization (PSO) and Henry's Gas Solubility Optimization (HGSO) have been utilized to optimize the SVR in finding some internal parameters. Different metrics were chosen to evaluate the performance of models. Consequently, the R2 in the testing stage for SVR-HGSO was computed at 0.90 and for SVR-PSO, 0.93. In the calibration phase, the correlation rate was computed at 0.93 for SVR-HGSO with a 3% difference from the SVR-PSO with 0.90.

1. Introduction

The Self-compacting concrete, known as SCC, is a novel type of high-performance concrete (HPC) characterized by the given ability for spreading into a location under its weight without the vibrations, accompanied by self-compacting without any segregation and blocking [1]. SCC has three crucial features: I) Filling capability, the concrete ability for flowing and filling the frameworks by their weight [2]; II) the passing ability, that is, the concrete ability for going through the congested gaps of reinforcing bars [3]; and III) Separation resistance is to the SCC capability to preserve the uniformity and homogeneity of concrete in concreting operation [4]. Using self-compacting concrete provides many advantages, including saving labor and equipment expenses, accelerating construction, allowing more flexibility in reinforcing bars, and smoother concrete surfaces [5]. Such extraordinary features of this concrete are created using supplementary cementitious materials consisting of slag cement, fly ash, silica fume, and superplasticizers (SPs) [6].

* Corresponding Author: Ling Chen
Email: st2@tzvtc.edu.cn

The presentation of SCC introduces a comprehensive technological advance in improving the quality of created concrete, making the concrete construction process faster and more economical. SCC was first produced in Japan 12 years ago and has been adopted in Europe, North America, and other countries. It would be possible to improve the quality of concrete, economic efficiency (improved casting speed and reduced labor, energy, and equipment costs), and Further development for automation of finished parts, by eliminating the compaction operation. Also, bringing up the significant improvements in working conditions (mass consumption of industries by products and reduction of health hazards and noise) [7]–[10].

The first generation of SCC used in the UK and Europe, such as the one developed in a large European research project, which investigated the practicability of using SCC in both civil engineering and in building structures, contained a high dosage of powder, as well as a high dosage of superplasticizer, to ensure adequate filling ability and passing abilities and segregation resistance [6]. Savings in labor costs might offset the increased cost related to the use of more cement and SP, but the use of mineral admixtures, such as pulverized fuel ash (PFA), ground granulated blast slag (GGBS) or limestone powder (LSP), could increase the fluidity of the concrete, without any increase in the cost. The incorporation of PFA or GGBS, or LSP reduced the requirement of SP necessary to obtain a similar slump flow compared with the same concrete containing only cement

Developed in a major European research project investigating the practicality of using SCC in architectural and structural engineering, the first-generation SCC used in the UK and Europe includes high doses of powder and superplasticizer (SP), ensuring sufficient filling and passage and resistance to separation [6]. Labor savings can compensate for the increasing costs of cement and SP, but mineral mixtures such as crushed fuel ash (CFA), ground granulated blast slag (GGBS), and limestone powder consequently, improve the fluidity of the concrete without increasing the cost. Incorporating CFA, GGBS, or limestone can reduce the amount of SP required to have a similar slump compared to the similar concrete containing only cement [6], [10], [11]. Mentioned additives also improved rheological variables [11], moreover, reducing the risk of concrete cracking due to heat of hydration and thus improved durability [12], [13]. Second-generation SCC with low powders like LSPs was studied using the design of experiments procedures that elaborate slump, V-funnel tests, rheological variables, settling, and compressive strength [14].

Adopting artificial intelligence (AI) techniques is a wide range of ways to solve technical problems and develop reliable models for predicting structural and material behavior. Various AI-based technologies have been used in various applications in civil engineering and building material performance, especially in appraising the compressive strength (CS) of concrete. Machine learning approaches with high-accurate abilities to model the key variables of dependent types are used in various researches [15], [16]. Support vector regression (SVR), a powerful branch of machine learning utilized in modeling CS seems successful in obtaining desirable assessment stage in a wide range of research projects [17]–[19]. The present article has attempted to model the CSs of 327 SCC samples by reproducing CS factors coupling with novel optimization algorithms of Particle Swarm Optimization (PSO) and Henry's Gas Solubility Optimization (HGSO). To help the SVR model, optimizers will find the determining variables to increase the accuracy and simultaneously reduce the cost of the modeling process. Hybrid PSO-SVR and HGSO-SVR fed by data will be capable of finding the SCC physical feature at a precise level examined via five metrics of R^2, *RMSE, VAF, OBJ,* and *MAE*.

2. Materials and Methodology

2.1.Preparation of initial dataset

Evaluation of the model developed in this study to evaluate the compressive strength of SCC experimental samples collected from research [20] is one of the main goals. SVR's powerful models try to model CS values where optimization algorithms can improve the quality of the model's results which processing dataset is an important step in achieving the specified goals. Using the BBO and FDA algorithms, SVR finds a better solution for calculating embedded variables within predictive models that cause hybrid BBO-SVR and FDA-SVR to estimate CS based on target values. For the current phase, 327 experimental samples were collected and brought up in Table 1.

Table 1. Specification of studied DGs.

Component	Cement	Water	Class F fly ash	Coarse Aggregate	Fine Aggregate	Superplasticizer	SCC sample age	Compressive Strength
Acronyms	C (kg/m3)	W (kg/m3)	CFFA (kg/m3)	CA (kg/m3)	FA (kg/m3)	SP (kg/m3)	Age (days)	CS (MPa)
Max	503.00	390.39	373.00	1190.00	1109.00	113.55	365.00	90.60
Min	61.00	132.00	20.00	590.00	434.00	0.00	1.00	4.44
Ave	293.08	197.00	170.23	828.34	807.47	23.15	44.31	36.45

St. Dev.	89.78	37.62	69.68	137.30	135.80	27.09	63.76	19.07

Moreover, mixing ingredients of each SCC sample with various dosages will create diverse CS values. Therefore, CS modeling is performed via hybrid intelligent solutions. In Fig. 1, the CSs are shown via the various combinations of the ingredients that each sample of SCC is shown via one string crossing different axes representing ingredients, finally reaching the axis of CS on the left side. Remarkably, the color of strings is to differentiate the samples.

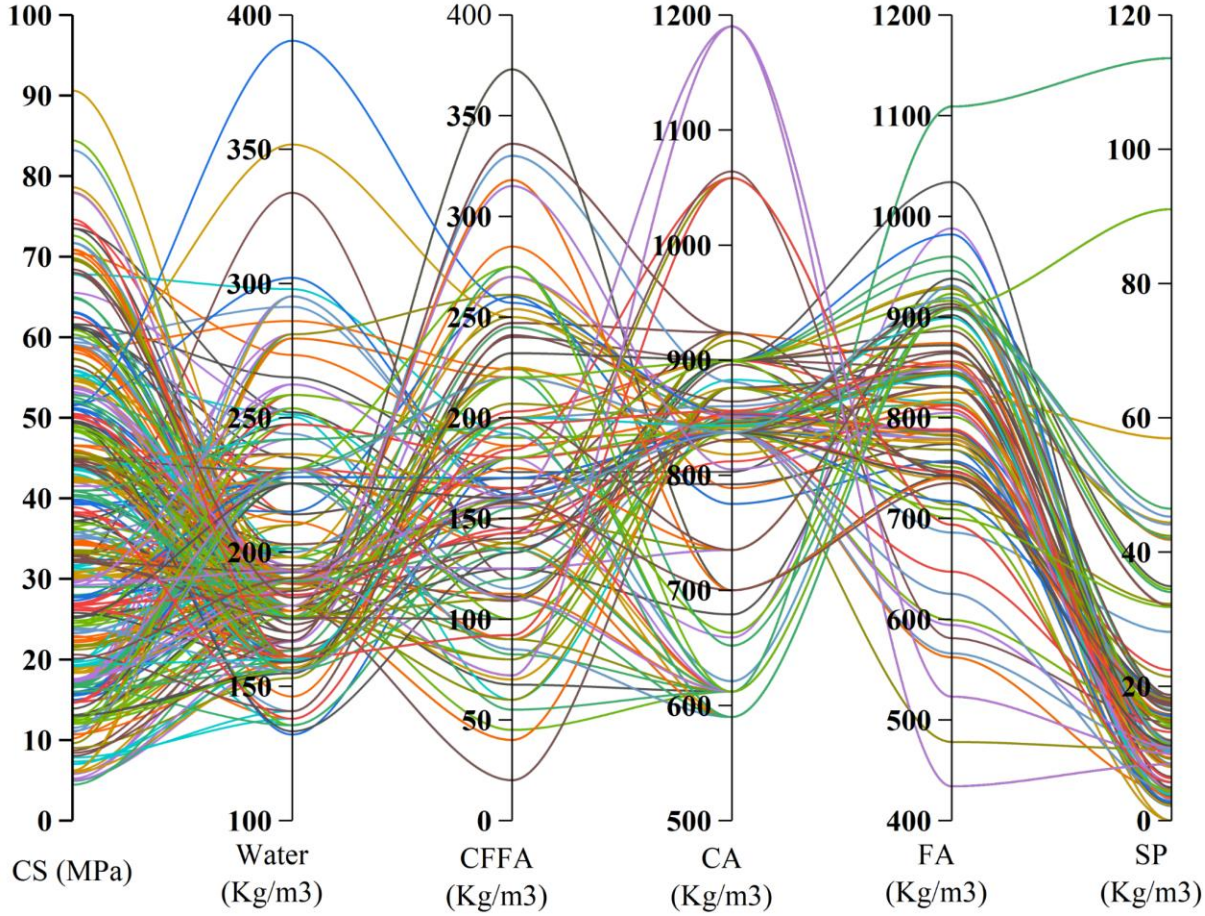

Fig. 1. The ingredients mixed in SCC samples and the target of CS

In this section, the main model of SVR computing the CS values is defined, and the optimization algorithms assistant of the main model accurately does its assigned task.

2.2. Support Vector Regression, SVR

The support vector machine, as a technique of machine learning, is designed to categorize the regression matters that are widely used in many studies [17], [18], [21]–[23]. The Support Vector Regression (SVR) uses the ε as the error area in defining a regression paradigm. It would be important that categorizing the classes of regressions can be done for defining hyperplane boundaries. Support Vector Regression used in the present article is supervised for establishing answers for the operation of regression that in Eq. (1) develops the attributes [24]:

$$min_{w,b} = \frac{1}{2}\|w\|^2 + C\sum_{i=1}^{m}(\xi_i + \xi_i^*),$$
$$const. \begin{Bmatrix} y_i - (w^T x_i + b) \le \varepsilon + \xi_i \\ (w^T x_i + b) - y_i \le \varepsilon + \xi_i^* \\ \xi_i, \xi_i^* \ge 0 \end{Bmatrix} \quad (1)$$

Where ξ represents the boundary violation amount; the parameter of y is the observed CS; regularizing parameter in a queue is shown by C; b shows the bias rate; w is considered for the factor weight; also, ε shows the deviation rate in the hyper-plane. Both terms in defined relation are elaborated as follows:

$$\frac{1}{2}\|w\|^2 \quad (2)$$

$$C\sum_{i=1}^{m}(\xi_i + \xi_i^*) \quad (3)$$

Eq. (2) presents the incremental gaps between the hyperplane boundaries and samples to create the area between the hyperplane boundaries and samples. Another relation (3) acts as a corrective tool. In these functions targeting the hyperplane, the w and b magnitudes will be estimated. Finally, the quadratic objective function used in this paper tries to find the parameters of support vector regression optimally, including $sigma$, C, and ε [25]. In light of mentioned contents, Fig 2 shows the flowchart of developed hybrid models.

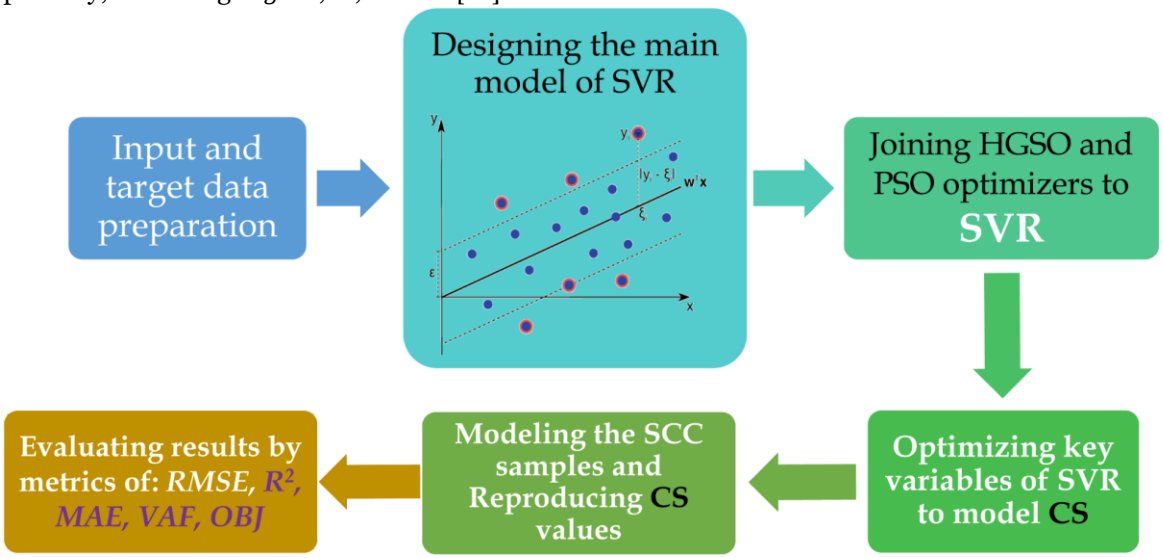

Fig. 2. Flowchart of hybrid models' mechanism

Based on Figure 2, When using raw model, performance of designed model can be influenced by choosing potential biased rates for arbitrary magnitudes of internal settings of main model, including $sigma$, C, and ε [25]. But in present research optimizing these numbers can increase the efficiency of common models in predicting compressive strength with high-accuracy modifications.

2.3. *Particle swarm optimization algorithm, PSO*

The Particle swarm optimization algorithm (PSO) is a population basis solution for solving problems [26], [27]. This method is created to consider the data swapping in animals societies. PSO was designed by Kennedy *et al.* in their research [28], widely cited by several papers [29]–[32]. Generally, the variable of position and velocity are remarkable items for population regulations. The scoring systems are considered to find the appropriate position on the local scale, and the best solution is defined as the best position for a global answer. The particles' velocity and position are calculated in compute epochs to reach the maximum iteration rate. The following equations lead the velocities and the locations to be upgraded.

$$P.v_{ij}^{new} = WP.v_{ij}^{current} + C_1 r_1 (P.p.best_{ij}^{new} P.p_{ij}^{current}) + C_2 r_2 (Global.best_{ij}^{current} - P.p_{ij}^{current}) \quad (4)$$

$$P.p_{ij}^{new} = P.p_{ij}^{current} + P.v_{ij}^{new} \quad (5)$$

In the above equations, W shows the inertia factor; $P.v$ and $P.p$ are the velocity of particles and the positions; The parameters of C_1 and C_2 denote the acceleration factors for local and global learning are calculated, alternatively;, The of r_1 and r_2 parameters represent the random magnitudes [0 – 1], and $Global.best$ shows the best solutions of all swarms.

2.4. *Henry's gas solubility optimization algorithm, HGSO*

Henry's gas solubility optimization (HGSO) has been constructed in terms of Henry's laws of physics [33]. According to the maximum amount of solute in the dissolved form, these rules were established at particular pressures and temperatures [34]. By applying the above the law, it is possible to prove the solubility of a sparingly soluble gas in a certain solvent. The key factors of temperature and pressure are the efficient factors for

solubility. For gases, this item is reduced by increasing the temperature, which is true for solids. In addition, pressure gradually leads to improved solubility [33], [35]. The following is an overview of the steps required for solving problems via HGSO.

a- Assigning the position and number of gas molecules (defining the initial population rate).
b- Assigning the classes of population as its type.
c- Assigning the cost classes and then routing the best answers scored for assigning the suitable conditions.
d- Recalculation of coefficients in Henry's law.

$$H_j(t+1) = H_j(t) \times e^{\left(-C_j\left(\frac{T^{\theta}-T(t)}{T(t)\times T^{\theta}}\right)\right)} \quad (6)$$

$$T(t) = e^{\left(\frac{t}{iter}\right)} \quad (7)$$

In the above equations, the H_j for class, j represents the coefficient for the Henry gas law.C_j and T^{θ} are the accidental and constant number in [zero - 1], respectively. In addition, the $iter$ and t parameters show, alternatively, the number of iterations in the queue and temperature.

e- Recalculation of the solubility by Eq. (8).

$$S_{i,j}(t) = K \times H_j(t+1) \times P_{i,j}(t) \quad (8)$$

In which K is a constant number; $P_{i,j}(t)$ and $S_{i,j}$ of gas i^{th} and the class of j represents, respectively, the parameters of pressure and solubility.

f- Consequently, the primitive population position is upgraded via the below relations.

$$X_{i,j}(t+1) = X_{i,j}(t) + F \times r \times \gamma \times \left(X_{i,best}(t) - X_{i,j}(t)\right) + F \times r \times \alpha \times \left(P_{i,j}(t) \times X_{best}(t) - X_{i,j}(t)\right) \quad (9)$$

$$\gamma = \beta \times e^{\left(-\frac{F_{best}(t)+\varepsilon}{F_{i,j}(t)+\varepsilon}\right)} + \varepsilon \quad (10)$$

For the above equations, γ represents the gases' interaction potential; the parameters $F_{i,j}$ and F_{best} represent the best cost in the gas i and cluster of population j; $X_{i,j}$ shows the i gas location in the j class; The $X_{i,best}$ and X_{best} variables are, respectively, the located gas in the class of j and the population. The r parameter also shows a random value in [0 to 1]. The fixed numbers of α and β will be considered 1 as well as ε= 0.05.

g- The lowest and worst gases are known for passing the local minimum trapping.

$$N_w = N \times (rand(C_2 - C_1) + C_1) \quad (11)$$

In Eq. (11), the N shows the population and the fixed numbers of C_1 and C_2 are assumed to be 0.1 and 0.2, respectively.

h- The location of the worst gas is obtained via the below relation.

$$G_{i,j} = G_{Min(i,j)} + r \times \left(G_{Max(i,j)} - G_{Min(i,j)}\right) \quad (12)$$

Where, $G_{i,j}$ parameter denotes the i gas position in j class; Moreover G_{Min} and G_{Max} variables represent the lower and upper boundary, respectively.

Examining the performance of HGSO-SVR and PSO-SVR models

For evaluating the developed models in terms of error rates involved in CS values, the five indices are used to examine the effectiveness of HGSO-SVR and PSO-SVR models in reproducing compressive strength (CS) of SCC samples specified in Table 2.

Table 2. Evaluating indices for assessment of model performance

Criteria name	Nomenclature	Relations	Assessment
Variance account factor	VAF	$\left(1 - \frac{\mathrm{var}(t_n - y_n)}{\mathrm{var}(t_n)}\right) * 100$ (13)	High is good
Mean absolute error	MAE	$\frac{1}{N}\sum_{n=1}^{N}\lvert p_n - t_n\rvert$ (14)	Low is good
Root mean squared error	RMSE	$\sqrt{\frac{1}{N}\sum_{n=1}^{N}(p_n - t_n)^2}$ (15)	Low is good
Pearson's correlation coefficient	R2	$(\frac{\sum_{n=1}^{N}(t_n - \bar{t})(p_n - \bar{p})}{\sqrt{[\sum_{n=1}^{N}(t_n - \bar{p})^2][\sum_{n=1}^{N}(p_n - \bar{p})^2]}})2$ (16)	High is good

Statistical parameters, including the various error indices	OBJ	$\left(\frac{n_{train}-n_{test}}{n_{train}+n_{test}}\right)\frac{RMSE_{train}+MAE_{test}}{R^2_{train}+1}+\left(\frac{2n_{train}}{n_{train}+n_{test}}\right)\frac{RMSE_{test}-MAE_{test}}{R^2_{test}+1}$ (17)	Low is good [20]

In Table 2, t_n represents CS measured target values; p_N refers to the compressive strengths estimated of SCC samples; The parameter of $\bar{t}$ is the CS measured averagely; $\bar{p}$ denotes the estimated compressive strength rates; Also, ntrain and ntest are the numbers of SCC samples for calibration and testing stages

3. Results and discussion

Creating developed hybrid models, the HGSO-SVR and PSO-SVR generated CS values based on input data of 327 SCC samples fed to models. In this process, the information on each ingredient was used to train the presented models. Moreover, the optimizers were used to find the optimum rate of key variables of SVR that Table 3 has shown them. On the other hand, the assessment criteria examined the SVR-HGSO and SVR-PSO results to reproduce the target values of CS. Firstly, the results of training each initial sample data were used to feed models, and in the testing phase, the capability of models was observed, which is discussed in this section.

.

Table 3. The SVR key variables' values optimized

		SVR-HGSO	**SVR-PSO**
Training phase	*C*	0.915	4.076
	EPSILON	78.006	370.707
	sigma	2.6	4
Testing Phase	*C*	3.024	3.253
	EPSILON	133.550	412.075
	sigma	1.680	4

All data of CSs for using in training, validating, and testing phases are shown in Fig. 3. It should be noted that about 70 percent of data were used in the training phase, and the remaining 30 percent were used for validating and testing phase equally. By replacement operation of data, it is clear that data in the various domains were utilized in each stage.

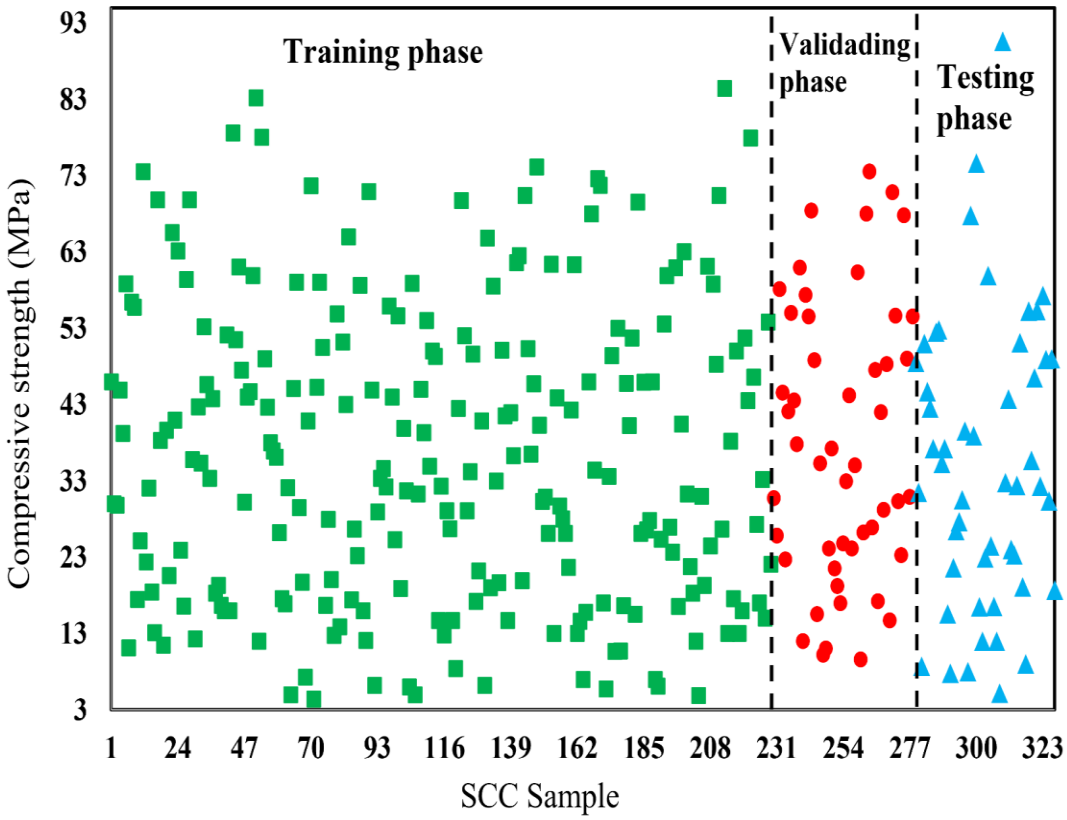

Fig. 3. All target data of models: compressive strength rates in different phases

The privilege of SCC to High-performance concrete (HPC) and traditional or typical concrete is for having the ingredient of superplasticizers (SP), fine aggregates (FA), and fly ash. In this regard, Fig. 4 shows the roles of each presented element in enhancing the CS factor. By surveying Fig. 4, they could be presented as three-dimension diagrams but are meaningless. The amount of given special materials appropriation to cement (C) to have high-resistant concrete is seeable. Based on Fig. 4, except for SP (c), other components positively affect the CS rate. While the SP at a high dosage leads to a decrease in the CS. Notably, the maximum value of CS happens at the low rate of given materials and the high rate of cement.

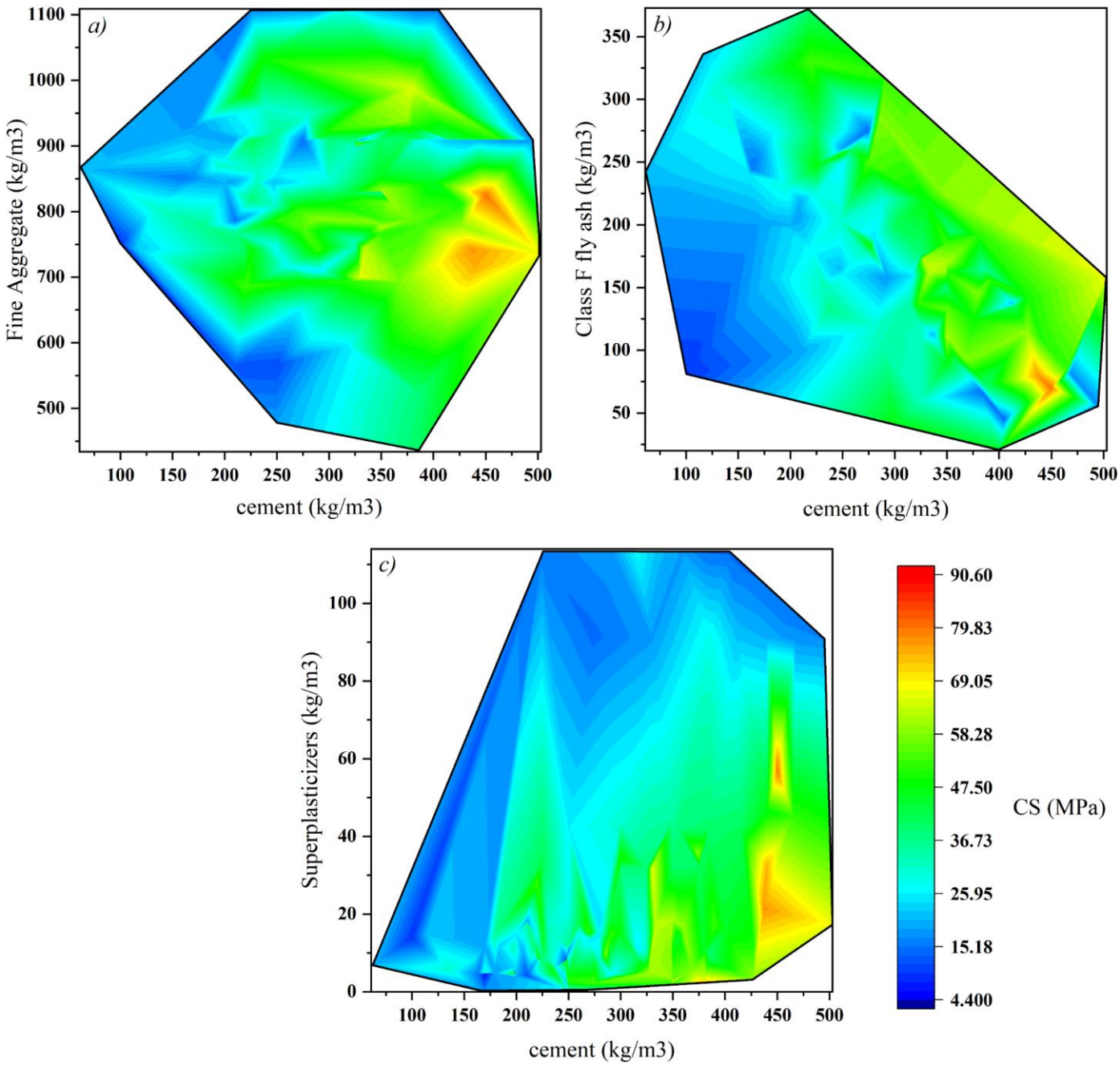

Fig. 4. Effect of composing cement with a) FA, b) fly ash, and c) SP on CS rate in SCC

During the modeling process, errors involved in computing CS should be highlighted, and the performance of models has to be analyzed. Concerning errors for each sample, Fig. 5 has exhibited the modeled compressive strength rates beside the target values as observed in experiments. According to Fig. 5, there are some points as samples that modeling trend and target line are not in same rates that this feature creates gaps between them. However, the condition for both HGSO-SVR (a) in the testing phase seems better. Fig. 6 shows the error rates involved in modeling CS for both developed frameworks to have a better view of modeling.

Regarding Fig. 6, the fluctuation of errors for both models in the testing phase seems harsher than in the training phase. However, the HGSO optimizer has smoothed the error graphs with high error rates of 61.28 percent, while for PSO, 94.76 percent. Nevertheless, the average error rate was obtained at 3.83% for HGSO-SVR and 7.91% for PSO-SVR.

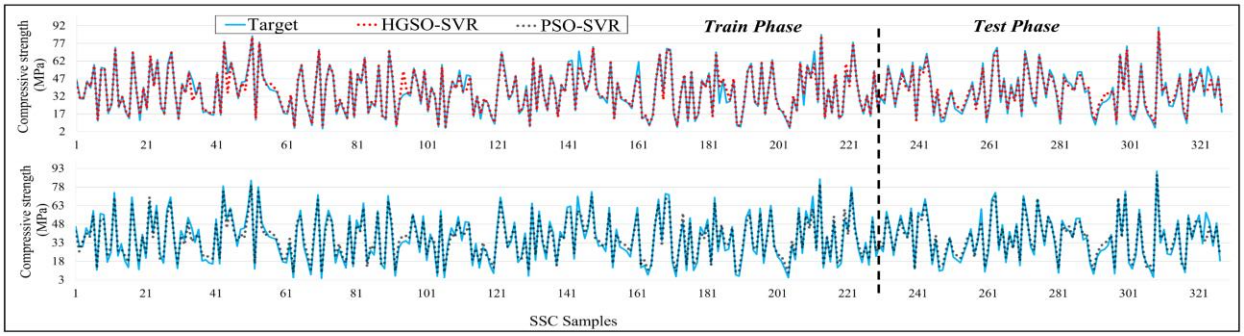

Fig. 5. The CS target value versus the CS values modeled via a) HGSO-SVR and b) PSO-SVR

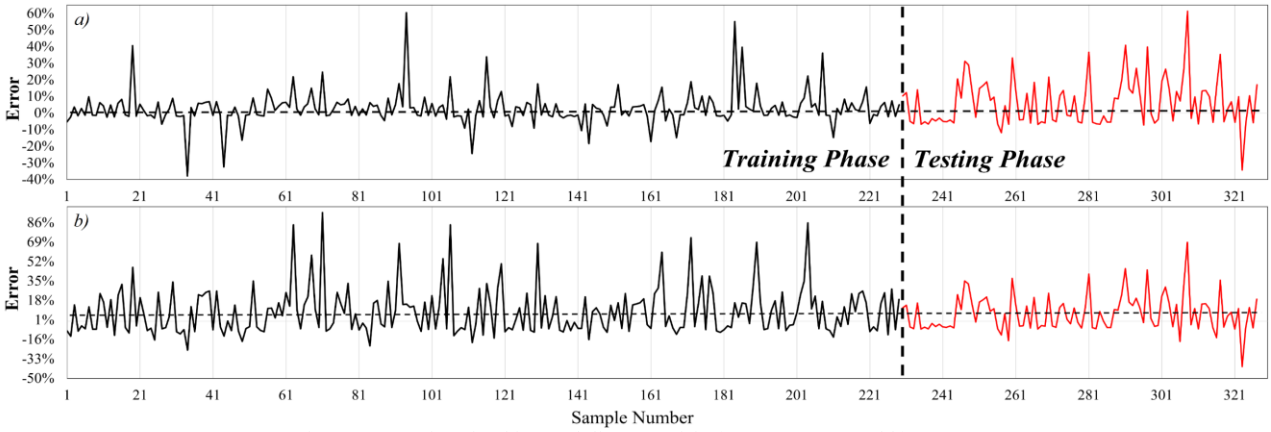

Fig. 6. Errors involved in modeling CS with a) HGSO-SVR and b) PSO-SVR

Trend lines through the CS values modeled for both frameworks also are exhibited using Fig. 7. According to the fitting line drawn through the CS points in both models, HGSO can generate accurate CS values near the target ones close to the bisector line rather than to PSO. The slope of the best-fit line of HGSO is 0.9 near to one, compared with PSO with a 0.85 slope rate. Noticing the distance of y=x bisector and best-fit line, it is definite that the gap between these mentioned lines for HGSO-SVR is small compared to PSO-SVR. However, there are some points in a distant area of the HGSO y=x bisector that this case for PSO is better. The overall condition of HGSO in spreading CS points around the bisector seems desirable compared to PSO.

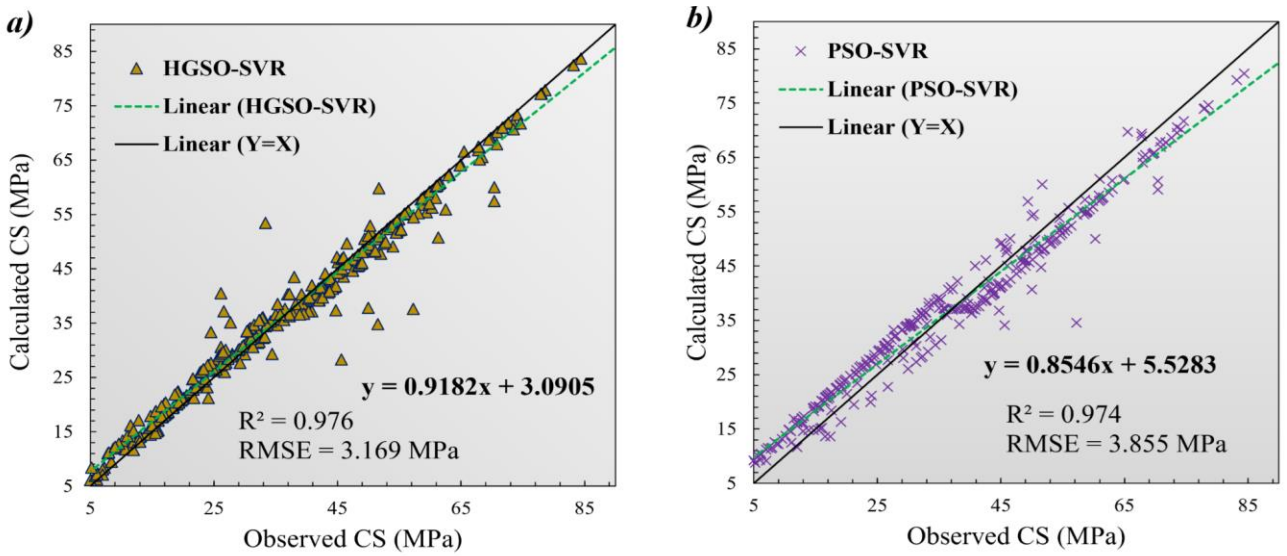

Fig. 7. CS rates are measured in front of estimated ones via the models of a) HGSO-SVR and b) PSO-SVR

Align with the previous figures and contents for examining the models' capability to manage errors, the five indices used to evaluate the models' performances are illustrated in Table 4 separately for the training and testing phases. Based on Table 4, the correlation index of R^2 for both models in both phases is the same, but the HGSO-SVR could obtain a little more than PSO-SVR, that the most difference belongs to the test phase with 0.78 percent for the better performance of HGSO algorithm. The error rate of models has a distinguishable discrepancy from the RMSE criterion. The largest difference between models for this index belongs to the training phase that HGSO-SVR, with a 23.31 percent difference, is placed in better condition with RMSE of 3.25 MPa while PSO-SVR was obtained at 4.01 MPa. The MAE of the training phase for the HGSO algorithm was estimated at the level of 1.7 MPa, and that of PSO-SVR was calculated at 3.71 MPa, more than two-fold of a former model. The VAF indicator also was calculated at 99.41 for PSO-SVR, 1.05% better than HGSO-SVR. Moreover, the OBJ index consisting of all correlation indexes, MAE, and RMSE was calculated at a better rate for HGSO with 39.19 percent.

Table 4. The results of metrics used to assess the models' performance

	Training step				**Testing step**				**Overall**
	R^2	*RMSE*	*MAE*	*VAF*	*R^2*	*RMSE*	*MAE*	*VAF*	*OBJ*
HGSO-SVR	0.9733	3.254	1.700	97.967	0.985	2.964	2.746	99.649	2.657
PSO-SVR	0.9727	4.012	3.715	99.393	0.977	3.459	3.206	99.522	3.698
Average	0.9730	3.633	2.707	98.68	0.981	3.211	2.976	99.585	3.177

In this part, the error distribution of developed models is indicated. Fig. 8 shows the distribution of errors according to their frequency rate and the curve of normal error distribution for SVR-PSO and SVR-HGSO. With this respect, there is no harmonic error distribution for each model.

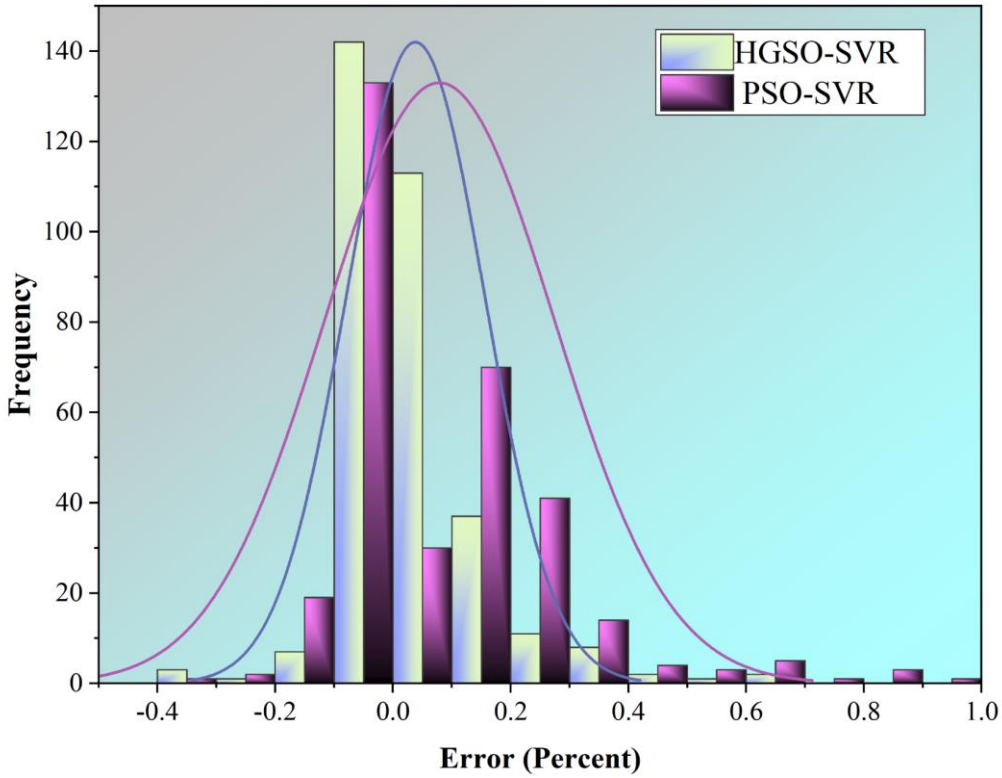

Fig. 8. The error distribution of models HGSO-SVR and PSO-SVR

That aggregation of error values near point zero creates the flat normal distribution curve of errors. Therefore, the concentration of errors in the SVR-HGSO model was better distributed as near-zero than in another model with a flat curve. Overall, the algorithm of HGSO

outperformed better than PSO according to the results of indices and figures shown.

4. Conclusions

Self-compacting concrete (SCC), as a liquid aggregate, is suitable for use in reinforced constructions with no need for vibration. The utilization of SCC has been found in a wide range of projects. Such extraordinary features of this concrete are created using supplementary cementitious materials consisting of slag cement, fly ash, silica fume, and superplasticizers (SPs). The presentation of SCC introduces a comprehensive technological advance in improving the quality of created concrete, making the concrete construction process faster and more economical. Nevertheless, most applications are often limited due to lacking the knowledge about such mixed materials, especially from experimental testing. The factor of Compressive Strength (CS), which is one of the vital mechanical variables in structure immunization, can be computed either through costly tests or predictive models. Intelligent systems can appraise CS based on ingredients' data fed to the models. Therefore, this research aims to model the CS of SCC via a machine learning technique of Support Vector Regression (SVR). Creating developed hybrid models, the HGSO-SVR and PSO-SVR generated CS values based on input data of 327 SCC samples fed to models. In this process, the ingredients information was used to train developed hybrid models.

Moreover, the optimizers were used to find the optimum rate of key variables of SVR to assist model the CSs accurately with low complexity of calculation. The R^2 of HGSO-SVR and PSO-SVR in both phases were the same, but the HGSO-SVR could obtain a little more rate than the latter one, that the most difference belonged to the test phase with 0.78 percent for HGSO-SVR. The model error rate had a definite difference in terms of the *RMSE* indicator. The largest difference between models for this *RMSE* belonged to the training stage; the HGSO algorithm was placed in better condition with a 23.31 percent difference for HGSO-SVR with RMSE of 3.25 MPa 4.01 MPa for PSO-SVR. The *MAE* of the training phase for the HGSO algorithm was estimated at the level of 1.7 MPa, and that of PSO-SVR was calculated at 3.71 MPa, more than two-fold of the former model. The *VAF* indicator also was calculated at 99.41 for PSO-SVR, 1.05% better than HGSO-SVR. In addition, the comprehensive criterion of *OBJ* consisting of all correlation indexes, *MAE*, and *RMSE* was calculated at a better rate for HGSO with 39.19 percent.

Generally, by using hybrid models and artificial intelligent-based models, accuracy of estimating compressive strength can be increase to substitute actual practical experiments as well as reducing the time and cost. Despite using optimization algorithms to regulate the function of models to predict some special parameters, the process of determining mentioned parameters can be done with entered bias due to many malfunctions of algorithms.

REFERENCES

[1] J. M. Khatib, "Performance of self-compacting concrete containing fly ash," *Constr Build Mater*, vol. 22, no. 9, pp. 1963–1971, 2008.

[2] A. Kandiri, E. M. Golafshani, and A. Behnood, "Estimation of the compressive strength of concretes containing ground granulated blast furnace slag using hybridized multi-objective ANN and salp swarm algorithm," *Constr Build Mater*, vol. 248, p. 118676, 2020.

[3] M. Serraye, S. Kenai, and B. Boukhatem, "Prediction of compressive strength of self-compacting concrete (SCC) with silica fume using neural networks models," *Civil Engineering Journal*, vol. 7, no. 1, pp. 118–139, 2021.

[4] İ. Özgür Deneme, "Modelling of compressive strength of self-compacting concrete containing fly ash by gene expression programming," *Revista de la construcción*, vol. 19, no. 2, pp. 346–358, 2020.

[5] M. Gesoğlu and E. Özbay, "Effects of mineral admixtures on fresh and hardened properties of self-compacting concretes: binary, ternary and quaternary systems," *Mater Struct*, vol. 40, no. 9, pp. 923–937, 2007.

[6] M. Sonebi and P. J. M. Bartos, "Filling ability and plastic settlement of self-compacting concrete," *Mater Struct*, vol. 35, no. 8, pp. 462–469, 2002.

[7] S. Nagataki and H. Fujiwara, "Self-compacting property of highly flowable concrete," *Special Publication*, vol. 154, pp. 301–314, 1995.

[8] K. Ozawa and H. Okamura, "Evaluation of self compactability of fresh concrete," 1995.

[9] P. J. M. Bartos and J. Cechura, "Improvement of working environment in concrete construction by the use of self–compacting concrete," *Structural Concrete*, vol. 2, no. 3, pp. 127–132, 2001.

[10] M. Sonebi, P. Bartos, and A. Tamimi, "Flexural response and performance of reinforced beams cast with self-compacting concrete," in *2nd International Symposium on Self-Compacting Concrete,* 2001.

[11] A. Yahia, M. Tanimura, A. Shimabukuro, Y. Shimoyama, and T. Tochigi, "Effect of mineral admixtures on rheological properties of equivalent self-compacting concrete mortar," in *Proc., 7th East Asia-Pacific Conf. on Structural Engineering and Construction*, 1999, vol. 21, pp. 559–564.

[12] R. Khurana and R. Saccone, "Fly ash in self-compacting concrete," *Special Publication*, vol. 199, pp. 259–274, 2001.

[13] K. H. Khayat, J. Bickley, and M. Lessard, "Performance of self-consolidating concrete for casting basement and foundation walls," *Materials Journal*, vol. 97, no. 3, pp. 374–380, 2000.

[14] A. Ghezal and K. H. Khayat, "Optimizing self-consolidating concrete with limestone filler by using statistical factorial design methods," *Materials*

Journal, vol. 99, no. 3, pp. 264–272, 2002.

[15] M. N. Amin, A. Iqtidar, K. Khan, M. F. Javed, F. I. Shalabi, and M. G. Qadir, "Comparison of Machine Learning Approaches with Traditional Methods for Predicting the Compressive Strength of Rice Husk Ash Concrete," *Crystals (Basel)*, vol. 11, no. 7, p. 779, Jul. 2021, doi: 10.3390/cryst11070779.

[16] W. Z. Taffese and E. Sistonen, "Machine learning for durability and service-life assessment of reinforced concrete structures: Recent advances and future directions," *Autom Constr*, vol. 77, pp. 1–14, May 2017, doi: 10.1016/j.autcon.2017.01.016.

[17] M. Shariati *et al.*, "A novel hybrid extreme learning machine–grey wolf optimizer (ELM-GWO) model to predict compressive strength of concrete with partial replacements for cement," *Eng Comput*, 2020, doi: 10.1007/s00366-020-01081-0.

[18] J.-S. Chou and A.-D. Pham, "Smart Artificial Firefly Colony Algorithm-Based Support Vector Regression for Enhanced Forecasting in Civil Engineering," *Computer-Aided Civil and Infrastructure Engineering*, vol. 30, no. 9, pp. 715–732, Sep. 2015, doi: 10.1111/mice.12121.

[19] L. Wang, *Support vector machines: theory and applications*, vol. 177. Springer Science & Business Media, 2005.

[20] G. Pazouki, E. M. Golafshani, and A. Behnood, "Predicting the compressive strength of self-compacting concrete containing Class F fly ash using metaheuristic radial basis function neural network," *Structural Concrete*, Feb. 2021, doi: 10.1002/suco.202000047.

[21] L. Wang, *Support vector machines: theory and applications*, vol. 177. Springer Science & Business Media, 2005.

[22] A. Al-Fugara, M. Ahmadlou, A. R. Al-Shabeeb, S. AlAyyash, H. Al-Amoush, and R. Al-Adamat, "Spatial mapping of groundwater springs potentiality using grid search-based and genetic algorithm-based support vector regression," *Geocarto Int*, pp. 1–20, 2020.

[23] K. Yan and C. Shi, "Prediction of elastic modulus of normal and high strength concrete by support vector machine," *Constr Build Mater*, vol. 24, no. 8, pp. 1479–1485, Aug. 2010, doi: 10.1016/j.conbuildmat.2010.01.006.

[24] V. Vapnik, *The nature of statistical learning theory*. Springer science & business media, 2013.

[25] A. Al-Fugara, M. Ahmadlou, A. R. Al-Shabeeb, S. AlAyyash, H. Al-Amoush, and R. Al-Adamat, "Spatial mapping of groundwater springs potentiality using grid search-based and genetic algorithm-based support vector regression," *Geocarto Int*, pp. 1–20, 2020.

[26] J. Wu, J. Long, and M. Liu, "Evolving RBF neural networks for rainfall prediction using hybrid particle swarm optimization and genetic algorithm," *Neurocomputing*, vol. 148, pp. 136–142, 2015.

[27] L. Xu, F. Qian, Y. Li, Q. Li, Y. Yang, and J. Xu, "Resource allocation based on quantum particle swarm optimization and RBF neural network for overlay cognitive OFDM System," *Neurocomputing*, vol. 173, pp. 1250–1256, 2016.

[28] R. Eberhart and J. Kennedy, "A new optimizer using particle swarm theory," in *MHS'95. Proceedings of the Sixth International Symposium on Micro Machine and Human Science*, pp. 39–43. doi: 10.1109/MHS.1995.494215.

[29] A. Maleki, "Optimal operation of a grid-connected fuel cell based combined heat and power systems using particle swarm optimisation for residential sector," *International Journal of Ambient Energy*, vol. 42, no. 5, pp. 550–557, Apr. 2021, doi: 10.1080/01430750.2018.1562968.

[30] G. Perampalam, K. Poologanathan, S. Gunalan, J. Ye, and B. Nagaratnam, "Optimum Design of Cold-formed Steel Beams: Particle Swarm Optimisation and Numerical Analysis," *ce/papers*, vol. 3, no. 3–4, pp. 205–210, Sep. 2019, doi: 10.1002/cepa.1159.

[31] F. Masoumi, S. Najjar-Ghabel, A. Safarzadeh, and B. Sadaghat, "Automatic calibration of the groundwater simulation model with high parameter dimensionality using sequential uncertainty fitting approach," *Water Supply*, vol. 20, no. 8, pp. 3487–3501, Dec. 2020, doi: 10.2166/ws.2020.241.

[32] M. B. Patil, M. N. Naidu, A. Vasan, and M. R. R. Varma, "Water distribution system design using multi-objective particle swarm optimisation," *Sādhanā*, vol. 45, no. 1, p. 21, Dec. 2020, doi: 10.1007/s12046-019-1258-y.

[33] F. A. Hashim, E. H. Houssein, M. S. Mabrouk, W. Al-Atabany, and S. Mirjalili, "Henry gas solubility optimization: A novel physics-based algorithm," *Future Generation Computer Systems*, vol. 101, pp. 646–667, Dec. 2019, doi: 10.1016/j.future.2019.07.015.

[34] V. Mohebbi, A. Naderifar, R. M. Behbahani, and M. Moshfeghian, "Determination of Henry's law constant of light hydrocarbon gases at low temperatures," *J Chem Thermodyn*, vol. 51, pp. 8–11, Aug. 2012, doi: 10.1016/j.jct.2012.02.014.

[35] T. L. Brown, *Chemistry: the central science*. Pearson Education, 2009.